PFC/RR-91-12

Beam and Viewing Dump Positioning Inside TFTR for CTS Alpha-Particle Diagnostics

D.Y. Rhee; P.P. Woskov
MIT Plasma Fusion Center

R. Ellis; H. Park
Princeton Plasma Physics Laboratory

July, 15 1991

This work was supported by DOE contract No. DE-FG-02-91ER-54109.

1 Introduction

A collective Thomson scattering (CTS) diagnostic system for localized measurement of energetic ions is being developed for TFTR[1]. This system will use a 200KW, 56GHz gyrotron and a sensitive heterodyne receiver. In addition, a key element of this system will be beam and viewing dumps which are needed to minimize detection of stray gyrotron and ECE background radiation by the receiver system. It is the purpose of this study to determine the size and location of these dumps inside TFTR taking into account beam refraction and launch and receiver antenna optics scanning.

The beam dump must cover all the area in the vacuum chamber where the beam is expected to impinge, and the viewing dump must cover all the areas within the direct line of sight of the receiver antenna. The beam launch system and the receiver antenna are to be placed nearly symmetrically above and below the midplane of the tokamak vacuum vessel, respectively. The beam dump is to be placed at the bottom inside of the vacuum vessel to absorb the gyrotron beam which will be launched from a top port. The viewing dump is expected to be placed symmetrically at the top inside of the vacuum vessel, and therefore a detailed analysis of only the beam dump is required here.

The beam dump must be robust enough to withstand the harsh environment near the fusion plasma, and it must be able to efficiently absorb the incident diagnostic millimeter-wave energy. Therefore the material selection of the dump is a very critical issue. However, the issue of the dump layout is the focus of this study and material selection issues are not covered. It is assumed that the best possible material will be selected for the beam dump design.

Since the 56GHz gyrotron radiation is expected to experience refraction in the TFTR plasma, an estimate must be made to adjust the straight line calculation done previously[2]. An outline of the method used to calculate the layout location of the beam dump is as follows.

- Starting with the experiment's scattering geometry in the tokamak, initial layout of the beam dump is calculated with the straight line assumption.
- Second, the refraction of the beams in the plasma is calculated using a ray tracing code to trace the rays around the perimeter of the diagnostic launch system scanning range.
- Third, the divergence of the beam is approximated by using a free space Gaussian beam calculation for each ray along the ray path.
- Finally, after adjusting for the divergence of the beam, intersection points of the rays with the vacuum vessel with adjustment made for the thickness of the beam dump are calculated to obtain the layout location of the beam dump.

In the following section, a brief description of the geometry of the CTS launch antenna system is presented. Then the ray tracing code used to calculate refraction of the beams is described. Assumptions made on the plasma model are also discussed in this section. Next, a discussion on the Gaussian optics follows, and the assumptions made to simplify the analysis are described. Then the method used to calculate the layout of the beam dump is discussed; and the result is presented and compared with the result obtained with the straight line calculation.

2 Beam Dump Positioning

The gyrotron beam will be launched downward from a top access port of the TFTR tokamak. Hence the beam dump must be placed at the bottom inside of the vacuum vessel. The optics for the launch beam are designed to be steerable in both toroidal and poloidal directions to allow for profile measurements and a reasonable range of scattering geometry. The steerable range of the antenna in the toroidal direction varies from $\xi = 0°$ to $10°$. In the poloidal direction, the antenna can be steered from

$\nu = 0°$ to $25°$ toward the outside of the torus. Because the steering optics will be located above the TFTR port, the poloidal pivot point is centered in this opening to maximize the diameter of the beam that can be transmitted. The toroidal pivot point for the optics is 5.5 inches above the poloidal pivot point to reduce the complexity of the mechanical steering system. The poloidal pivot point is 50 inches from the plasma midplane. The beam launch coordinate in the Cartesian system centered at the tokamak center is given by:

$$(102.599", 5.5\tan\xi", 50.0").$$

See Figure 1 for the layout diagram of the CTS system depicting the location of the launch point and the beam dump. The sweep range of the launch antenna in poloidal and toroidal direction is also illustrated in the figure.

3 Ray Tracing Model

The refractive effects of millimeter-wave beam propagation in a plasma are modeled by a geometric optics ray tracing code, RAYS[3]. Several modifications have been made to the RAYS code to model the toroidal equilibrium for a circular or an elongated plasma with simple but realistic analytic equations. The code can analytically model the magnetic shifts and the density profiles from experimental data. The following equation is used to model the flux of an elongated plasma.

$$\left(\frac{\psi}{\psi_\circ}\right)^2 = \left[\left(\frac{x}{a}\right) - \Delta(x,y)\right]^2 + \left[1+\delta\left(\frac{x}{a}\right)\right]\left(\frac{y}{\kappa a}\right)^2, \quad (1)$$

$$\Delta(x,y) = \delta_m - \delta_m\left\{\left(\frac{x}{a}\right)^2 + \left[1+\delta\left(\frac{x}{a}\right)\right]\left(\frac{y}{\kappa a}\right)^2\right\}. \quad (2)$$

Here, the ratio $\psi/\psi_\circ$ is the normalized flux, x and y are the plasma's horizontal and vertical Cartesian coordinates, a is the minor radius, δ is the plasma triangularity, κ

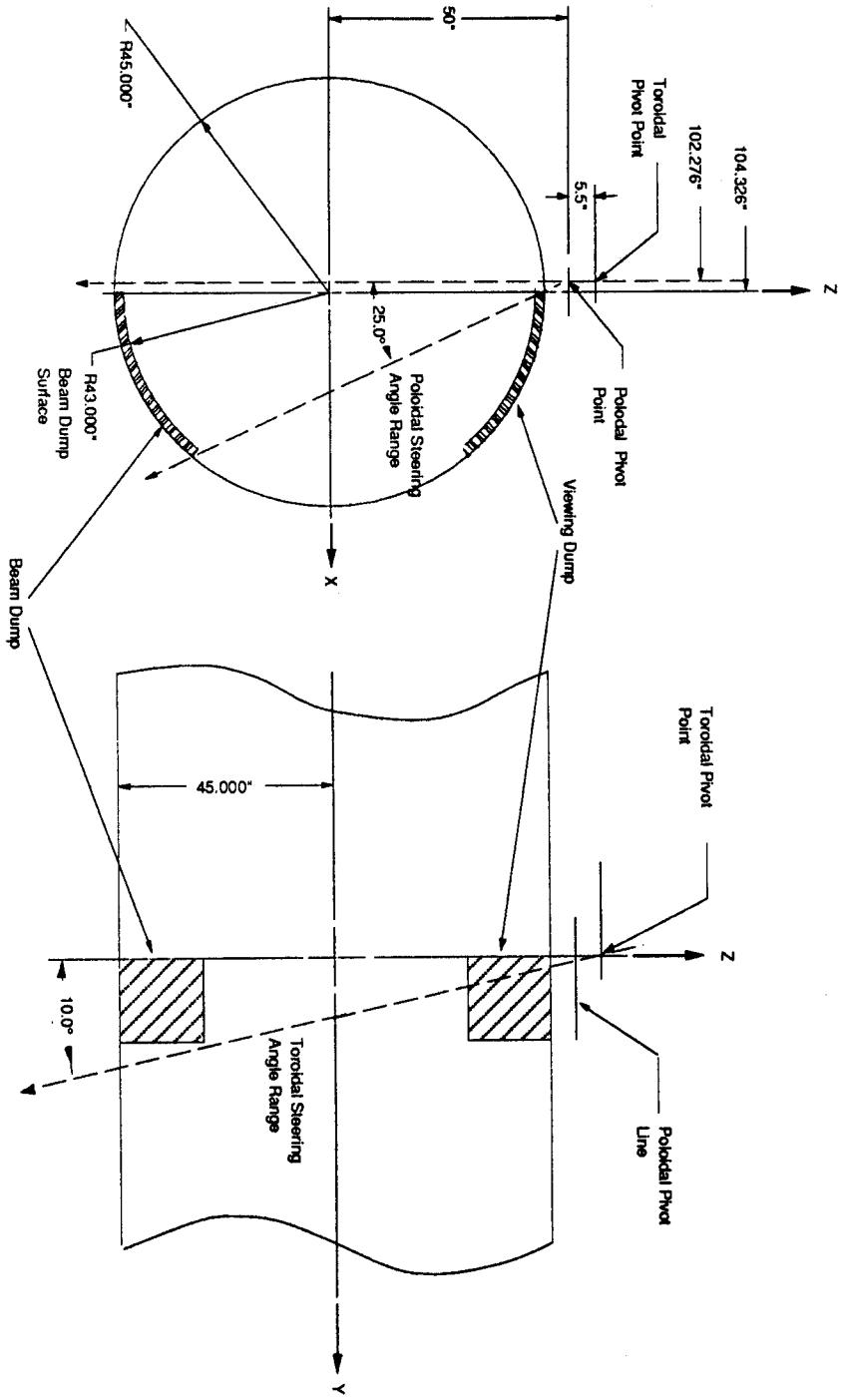

Figure 1: Schematic of the TFTR beam and viewing dump locations

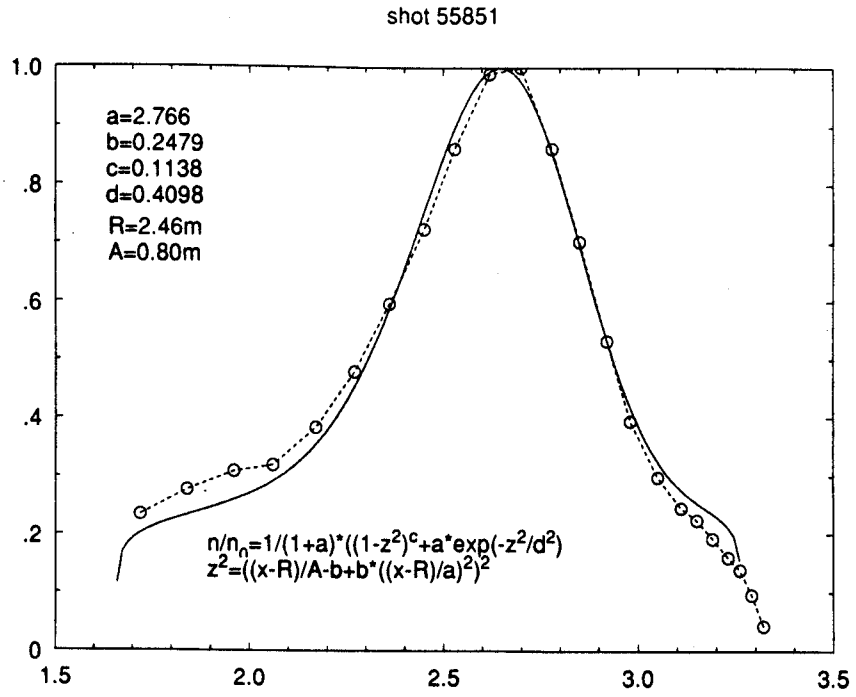

Figure 2: Density profile of the TFTR 'supershot' plasma: the dashed line is the experimental data, and the solid line is the curve fit.

is the plasma elongation, and δ_m is the magnetic shift. Values of $\delta = 0.0$, $\delta_m = 0.25$, and $\kappa = 1$ were used to model the TFTR plasma (Figure 2).

To model the exponential density profile observed in the TFTR 'Supershot' data, the density profile is modeled by the sum of a parabolic and an exponential profile:

$$\frac{n(x,y)}{n_o} = \left(\frac{1}{1+A}\right)\left\{\left[1-\left(\frac{\psi}{\psi_o}\right)^{p1}\right]^{p2} + Aexp\left[-\frac{(\psi/\psi_o)^2}{r_g^2}\right]\right\}, \qquad (3)$$

where n/n_o is the normalized density and A is the ratio of peak parabolic density to the peak exponential density; and $p1$, $p2$, and r_g are the shape parameters that determine the shape of the density profile. To determine the parameters of this model, a least squares fit to the experimental density profile is done with the above models of normalized flux and density profile. For the current analysis, TFTR's 'Supershot' experimental data (shot # 55851) is used[5].

Because the beam launch point is in the vacuum region, a straight line extrapolation from the launch point to the plasma boundary is done to calculate the initial ray

tracing launch points for various given launch angles. Also, once the ray tracing code has calculated the propagation of the rays in the plasma, another linear extrapolation is done from the plasma edge to the beam dump. Linear extrapolation of the ray in the region outside the plasma is valid because the ray does not refract in vacuum. The reason for doing a straight line extrapolation outside the plasma is that the ODE subroutine in the ray tracing code does not converge in the very low density region (ie. outside the plasma).

4 Gaussian Optics

To account for the finite diameter of the beam and divergence, a free space Gaussian optics calculation was used to approximate the beam width at the beam dump. Beam dump design must account for the widening of the beam to effectively minimize reflections In reality, the Gaussian optics assumption is not generally valid for a beam that experiences refraction because of non uniformity across its cross section. However, a zeroeth order analysis was made here by assuming that the refraction of the beam and beam divergence are separable. Hence, it was assumed that the plasma only affects the beam refraction; and it was further assumed that the beam divergence is governed by Gaussian optics along the ray path. With the following equation, the Gaussian beam radius of the ray at $1/e^2$ power can be calculated at any point along the beam path. The beam radius, w is given by

$$w = w_o \left[1 + \left(\frac{Z}{Z_R}\right)^2\right]^{\frac{1}{2}}, \tag{4}$$

$$Z_R = \frac{\pi w_o^2}{\lambda_i}, \tag{5}$$

where Z is the distance from the beam waist, Z_R is the Rayleigh range, λ_i is the incident beam's wavelength, and w_o is the beam waist[4]. The primary parameter in determining the beam divergence is the diagnostic port clear aperture. This port

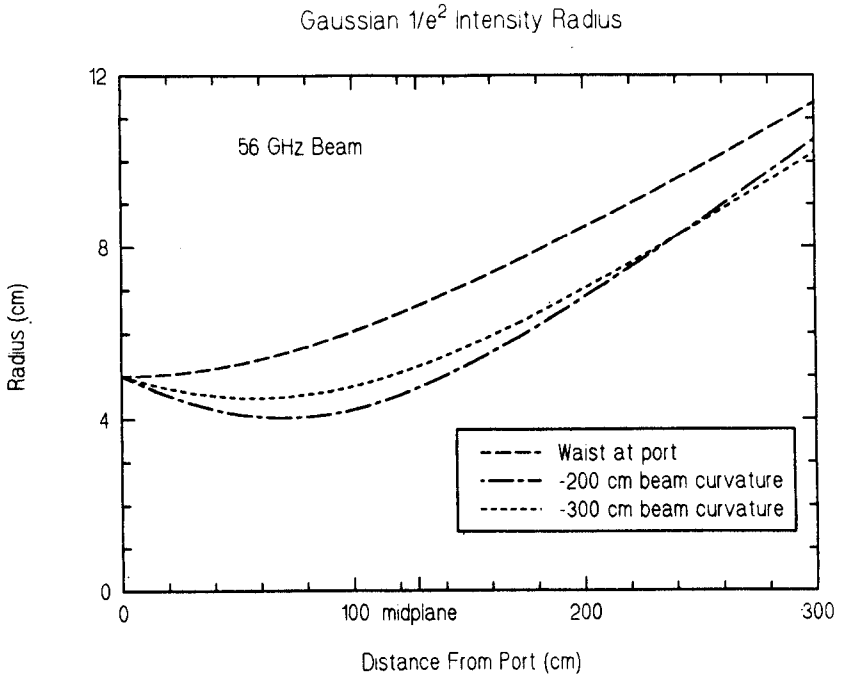

Figure 3: 5.35mm wavelength gaussian beam divergence plot. Note that even at 3 meters from the waist, the beam radius is still less than 12cm.

which has a diameter of 8", has an effective clear aperture of only 6" because of the need to offset the gyrotron beam for the toroidal scan. To avoid significant fringing the beam waist at the port must be chosen such that $a \geq 1.5$ w, where a is the port clear aperture diameter. Figure 3 illustrates the divergence of a 56GHz Gaussian beam restricted to w =5cm at the diagnostic port with the beam wavefront curvature at the port. Note for all these cases the beam radius at 300cm from the port is less than 12cm. For the present analysis, the beam diameter at the beam dump for all the rays has been conservatively assumed to be 9 inches.

In order to determine the location of beam dump edges that would extend far enough to take both beam refraction and beam divergence into account, the perimeter defined by the ray tracing code is adjusted for the finite beam width. This is done because the ray tracing code only calculates the propagation of the center ray of the beam. In the upper toroidal boundary, $\frac{d}{2\cos\nu}$ is added to the y direction (d is the beam diameter). In the lower toroidal boundary, $\frac{d}{2}$ is subtracted in the y direction. In the

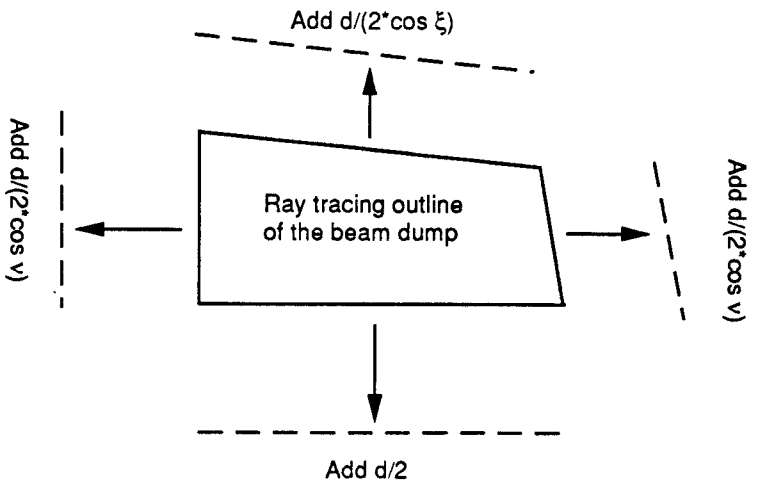

Figure 4: Schematic of adjustments made to the ray tracing outline of the beam dump to account for the beam diameter.

poloidal boundaries, $\frac{d}{2\cos\xi}$ is added and subtracted in the x direction at the right and left boundaries, respectively. See Figure 4.

After the adjustments are made to the ray tracing results to take the beam divergence into account, the rays are then linearly extrapolated down to the vacuum vessel to determine the beam dump perimeter. The direction of each ray is calculated by using the last two points, (x_1, y_1, z_1) and (x_o, y_o, z_o), of the ray after it emerges from the plasma. Assuming that the ray travels in a straight direction in the region outside the plasma, the two direction angles, α and β are calculated.

$$\alpha = Tan^{-1}\left[\frac{(y_1 - y_o)}{(x_1 - x_o)}\right], \tag{6}$$

$$\beta = Tan^{-1}\left\{\frac{[(x_1 - x_o)^2 + (y_1 - y_o)^2]^{1/2}}{(z_1 - z_o)}\right\}. \tag{7}$$

α and β correspond to the angles in the toroidal and poloidal directions, respectively.

The intersection points of the extrapolated rays with the effective vacuum vessel wall give the layout coordinates of the beam dump. Given the angles α, β of the beam

direction as given above and the last point of the ray right after passing through the plasma (x_o, y_o, z_o), the intersection point (x, y, z) between the ray and the dump that define the dump layout can be calculated with the following equations.

$$x = (z - z_o)\sin\beta\cos\alpha + y_o, \tag{8}$$

$$y = (z - z_o)\sin\beta\sin\alpha + x_o, \tag{9}$$

$$\phi = \tan(y/x), \tag{10}$$

$$s^2 = r_o^2 - (x - R_o\cos\phi)^2 + (y - R_o\sin\phi)^2 + z^2. \tag{11}$$

Above equations are solved iteratively for $s = 0$ with an initial guess of z. The solution of the intersection points defines the boundary of the beam dump layout that covers a large enough area to allow refracted beams to be absorbed by the dump.

5 Interpretation of Results

Figures 5, 6, and 7 show plots of the outlines of the beam dump from three perspectives. Results from straight line calculations and from ray tracing calculations are shown on the figures to compare the differences between the two calculations. See the appendix for the tables of the coordinates shown on the figures.

In the areas where the rays go through high plasma density regions, refraction is significant. Therefore the dump area, located directly below the central plasma region as viewed from the launch position, must be enlarged to accommodate for refraction of the beams. In contrast, in the areas where the rays do not go through dense plasma regions, no modifications are needed since the rays go through the plasma without any refraction.

As described from the perspective of the Figure 5 (viewing from the top, looking down to the plasma), the upper region of the dump needs to be enlarged the most to adjust for the refraction. Also, since the location of the peak plasma density is to the right side of the launch position, the beam refracts away from the central peak into

the inboard side of the vacuum vessel. Therefore, the left side of the dump also must be enlarged. If the beam is directed in such a way so that the ray always refracts to the outboard direction, then the left side of the dump does not need to be enlarged as much. Hence, if the ray is launched with poloidal steering angle (ν) of greater than a few degrees, then the dump locations on the left side do not need to be modified from the straight line calculations. At the bottom and the right side of the dump, no modifications seem to be necessary since the results from the straight line calculations and the ray tracing calculations overlap. In the bottom side, the rays refracted only in the poloidal direction and not in the toroidal direction because the rays were launched in the direction closely perpendicular to the magnetic field direction.

In conclusion, modifications to the beam dump layout due to refraction need to be made only on the upper and left sides (toroidal in direction of steering and inward radially) of the dump locations. These locations correspond to beam propagation directions where the beams experience refraction. On the lower and right sides of the dump, no modifications are needed because the beams that reach here do not refract noticeably.

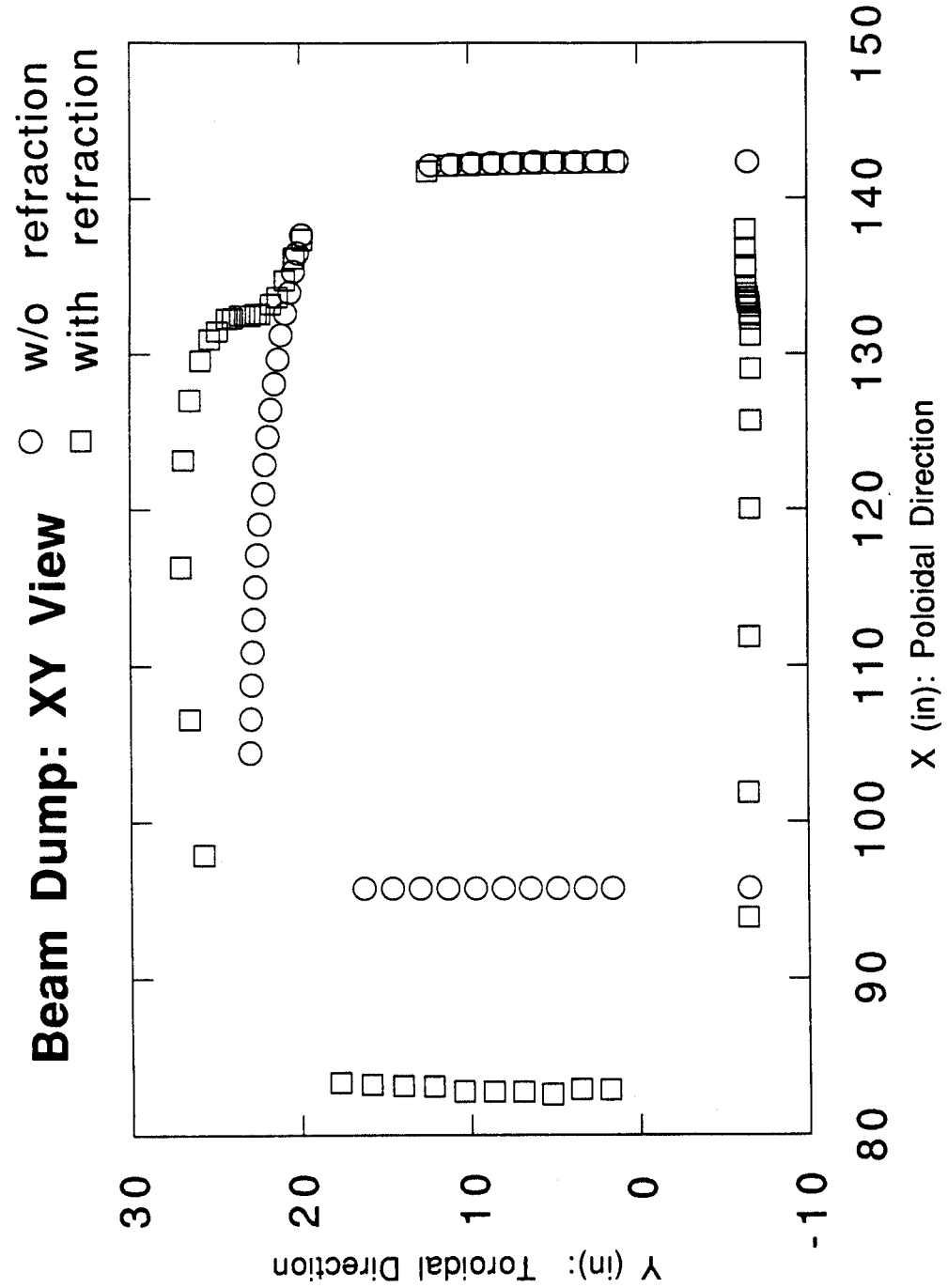

Figure 5: Beam dump: Top view: XY view

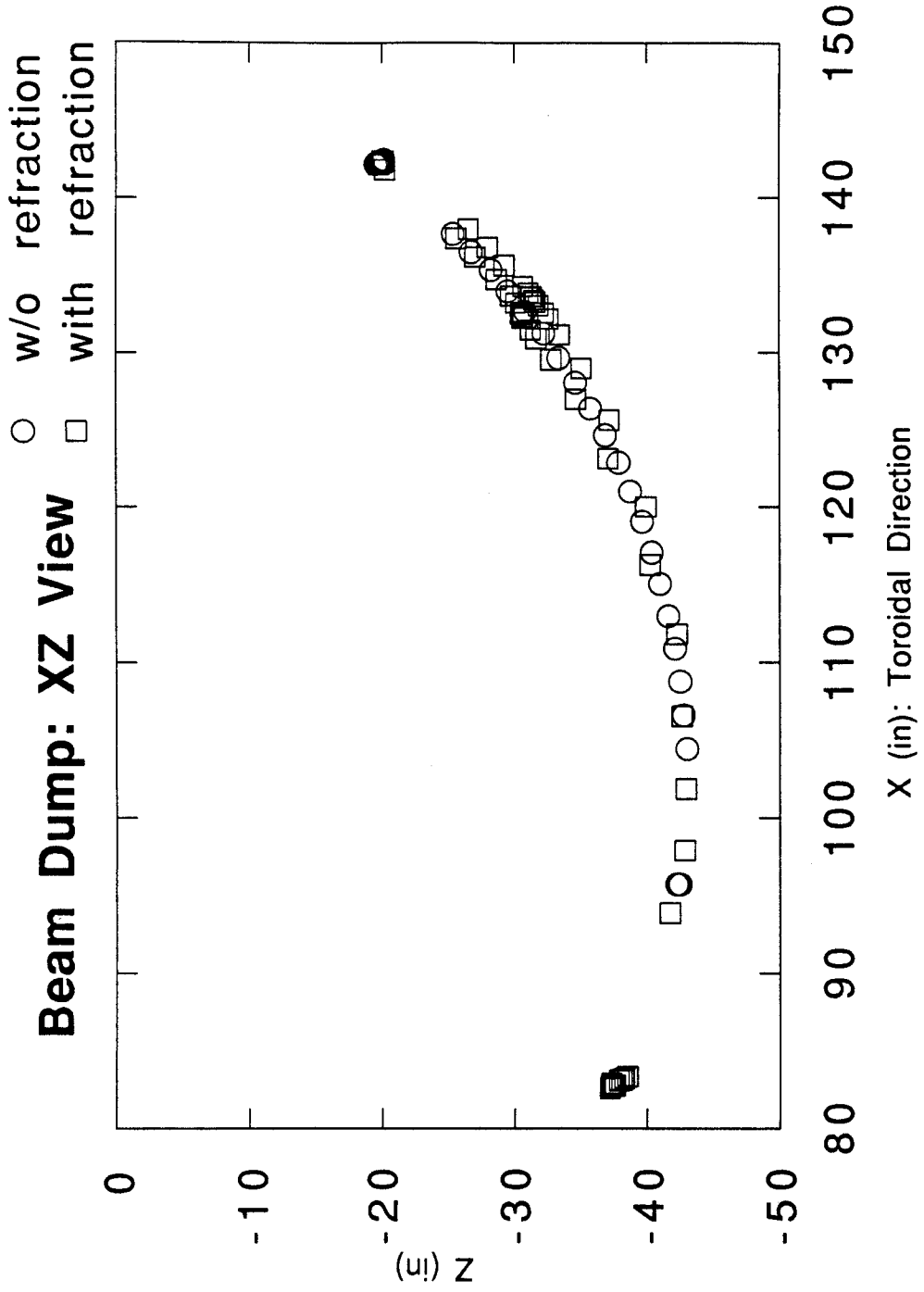

Figure 6: Beam dump: Side view: XZ view

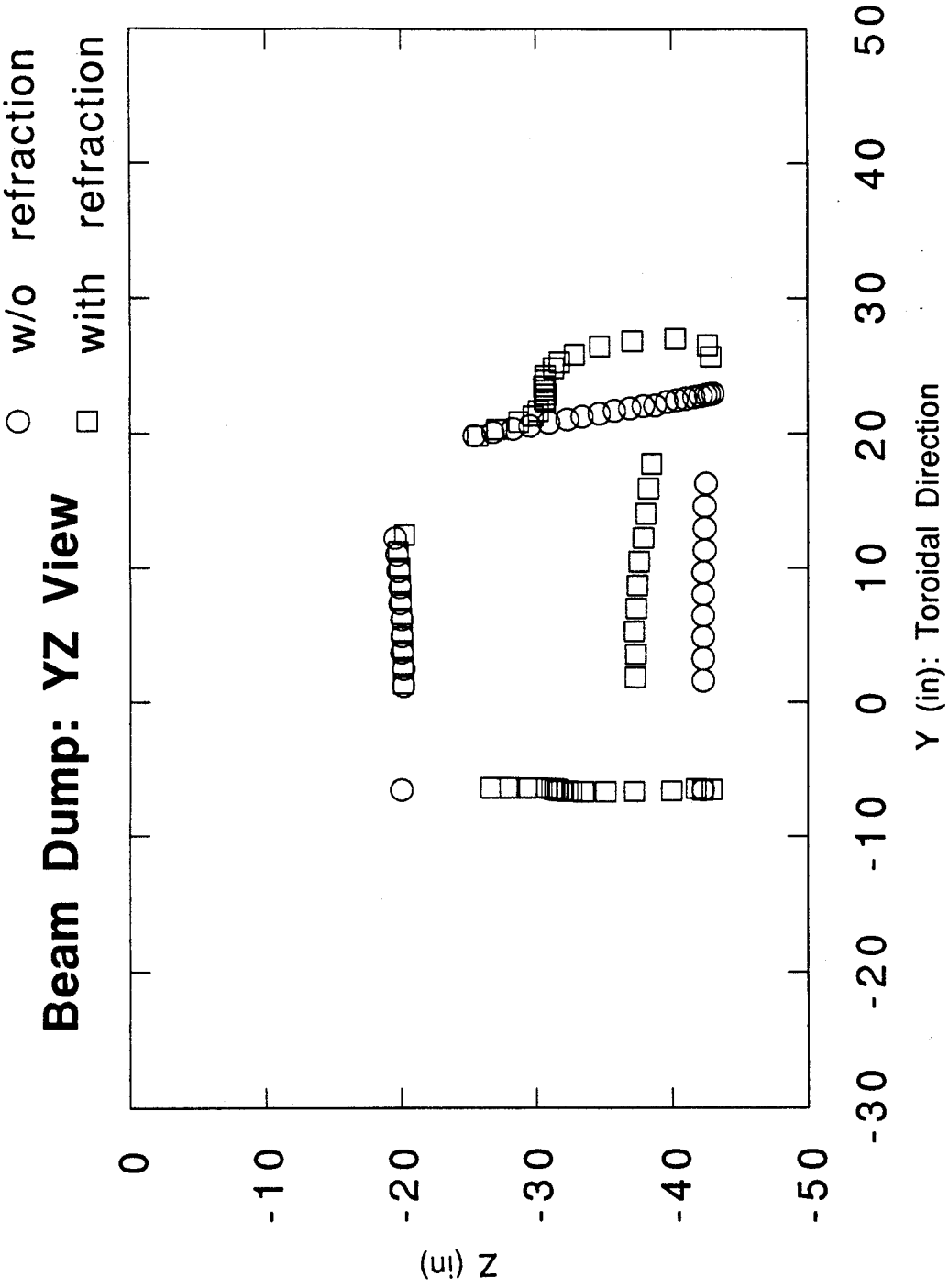

Figure 7: Beam dump: Side view: YZ view

A Appendix

With ray tracing		
x'	y'	z'
97.913	25.717	-42.874
106.57	26.551	-42.638
116.34	27.035	-40.276
123.19	26.862	-37.098
127.05	26.465	-34.677
129.57	25.858	-32.827
130.94	25.311	-31.705
131.50	24.854	-31.295
132.28	24.303	-30.657
132.32	23.945	-30.657
132.52	23.516	-30.543
132.52	23.240	-30.606
132.48	22.925	-30.709
132.64	22.583	-30.587
132.60	22.366	-30.685
133.23	21.717	-30.157
133.70	21.319	-29.752
134.76	20.886	-28.697
136.22	20.339	-27.075
137.40	19.850	-25.646
93.898	-6.4331	-41.772
101.89	-6.4882	-42.953
111.85	-6.5591	-42.283
120.04	-6.6220	-39.961
125.71	-6.6654	-37.213
129.02	-6.6811	-35.098
131.18	-6.6772	-33.461
132.20	-6.6575	-32.606
132.60	-6.6339	-32.268
133.07	-6.6063	-31.850
133.31	-6.5748	-31.626
133.31	-6.5472	-31.642
133.43	-6.5157	-31.500
133.66	-6.4921	-31.303
133.62	-6.4685	-31.350
133.90	-6.4291	-31.094
134.29	-6.4016	-30.709
135.67	-6.3858	-29.272
136.81	-6.3701	-28.016
137.99	-6.3661	-26.567
142.32	1.3547	-20.110
142.32	2.5795	-20.091
142.28	3.8146	-20.098
142.28	5.0512	-20.024

With ray tracing		
x'	y'	z'
142.24	6.2598	-20.004
142.20	7.5118	-19.972
142.17	8.7126	-19.902
142.13	9.9646	-19.843
142.09	11.213	-19.756
141.73	12.476	-20.217
82.874	1.8126	-37.283
82.913	3.5276	-37.327
82.598	5.2362	-37.209
82.756	6.9685	-37.354
82.756	8.6929	-37.449
82.795	10.476	-37.591
83.110	12.252	-37.886
83.150	14.067	-38.059
83.228	15.933	-38.272
83.346	17.776	-38.516

Straight line calc.		
x0	y0	z0
95.776	-6.5000	-42.250
142.36	-6.5000	-20.000
95.776	1.6100	-42.250
142.42	1.2240	-20.125
95.776	3.2210	-42.250
142.42	2.4490	-20.125
95.776	4.8350	-42.250
142.36	3.6690	-20.000
95.776	6.4510	-42.250
142.36	4.8950	-20.000
95.776	8.0710	-42.250
142.36	6.1240	-20.000
95.776	9.6960	-42.250
142.30	7.3440	-19.875
95.776	11.342	-42.375
142.30	8.5800	-19.875
95.776	12.982	-42.375
142.24	9.8030	-19.750
95.776	14.631	-42.375
142.18	11.028	-19.625
95.776	16.310	-42.500
142.12	12.255	-19.500
104.46	22.999	-43.000
106.64	22.955	-42.750
108.80	22.911	-42.500
110.94	22.844	-42.125
113.04	22.756	-41.625
115.11	22.646	-41.000
117.14	22.536	-40.375
119.13	22.404	-39.625
121.05	22.149	-38.750
122.93	22.095	-37.875
124.73	21.919	-36.875
126.46	21.720	-35.750
128.13	21.522	-34.625
129.71	21.302	-33.375
131.27	21.103	-32.250
132.68	20.861	-30.875
134.04	20.618	-29.500
135.38	20.398	-28.250
136.54	20.133	-26.750
137.70	19.891	-25.375

Table 1: Beam dump layout coordinates with straight line calculations(x0,y0,z0) and with ray tracing calculations(x',y',z'). All dimensions are in centimeters.

References

[1] P. Woskov, J. Machuzak, D. Rhee, D. Cohn, N. Bretz, P. Efthimion, and H. Park, *First Workshop on Alpha Physics in TFTR*, March 28-29, 1990, Princeton Plasma Physics Laboratory

[2] R. Ellis, Princeton Plasma Physics Laboratory, (private communications) (1991)

[3] D.B. Batchelor, R.C. Goldfinger "RAYS: A Geometrical Optics Code for EBT" ORNL/TM6844 (1982)

[4] J.D. Gaskill Linear Systems, Fourier Transforms, and Optics, John Wiley and Sons, Inc. (1978)

[5] H. Park, Princeton Plasma Physics Laboratory (private communications) (1991)